Jurnal Teknologi

Full Paper

PARAMETRIC STUDY OF WEB-POST BUCKLING FAILURE ON PROTECTED COMPOSITE CELLULAR STEEL BEAM (CSB) AT ELEVATED TEMPERATURE

Renga Rao Krishnamoorthy[a,b], Fariz Aswan Ahmad Zakwan[b]*, Ruqayyah Ismail[b], Azmi Ibrahim[b]

[a]Smart Manufacturing Research Institute (SMRI), Universiti Teknologi MARA, 40450 Shah Alam, Selangor, Malaysia
[b]School of Civil Engineering, College of Engineering, Universiti Teknologi MARA, 40450 Shah Alam, Selangor, Malaysia

Article history
Received
10 October 2023
Received in revised form
22 December 2024
Accepted
7 January 2024
Published Online
20 February 2025

*Corresponding author
fariz838@uitm.edu.my

Graphical abstract

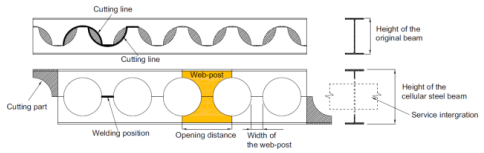

Abstract

Cellular Steel Beam (CSB) are Widely recognized and used in steel structures due to their numerous benefits, including visually appealing design, flexible structural elements, exceptional structural integrity, and the ability to incorporate utility conduits within the web beam section. These beams are often integrated into construction systems, often requiring the alteration of solid steel beams through the introduction of web holes to preserve their structural integrity. This study investigates the various forms of CSB failure that may arise from the insertion of circular web holes. High temperatures are a significant environmental factor that significantly impacts the performance of CSB, with failure modes associated with elevated temperatures including Vierendeel bending, web-post buckling, and vertical deformation. The study uses extensive finite element simulations with the ABAQUS program to numerically simulate and investigate the performance of shielded CSB with web apertures under increased temperature conditions and applied stresses. The study presents a novel methodology involving the use of intumescent coatings with different thicknesses to provide complete coverage of the CSB, aiming to improve the stiffness of the beam when exposed to high temperatures. The simulation findings show that the use of thicker intumescent coatings leads to marginal enhancements in the reduction of vertical deformation and web-post buckling. These findings are of practical significance for professionals in structural engineering and architecture involved in designing and evaluating structures based on composite steel and concrete materials in fire-prone areas, contributing to the advancement of resilient structural engineering.

Keywords: Vertical deformation, web-post buckling, intumescent coatings, fire, finite element simulation, steel structures

Abstrak

Cellular Steel Beam (CSB) secara meluas diiktiraf dan digunakan dalam struktur keluli kerana banyak faedah mereka, termasuk reka bentuk yang menarik secara visual, elemen struktur yang fleksibel, integriti struktural yang luar biasa, dan keupayaan untuk menggabungkan saluran utiliti dalam bahagian web beam. Beam ini sering digabungkan ke dalam sistem pembinaan, sering memerlukan perubahan beam keluli padat melalui pengenalan lubang web untuk mengekalkan integriti struktur mereka. Kajian ini mengkaji pelbagai bentuk kegagalan CSB yang mungkin timbul daripada penyisipan lubang web bulat. Suhu yang tinggi adalah faktor persekitaran

yang penting yang memberi kesan yang signifikan kepada prestasi CSB, dengan mod kegagalan yang dikaitkan dengan suhu yang tinggi termasuk menggeleng Vierendeel, web-post buckling, dan deformasi vertikal. Kajian ini menggunakan simulasi elemen akhir yang luas dengan program ABAQUS untuk mensimulasikan dan menyiasat prestasi CSB yang dilindungi dengan lubang web di bawah keadaan suhu yang meningkat dan tekanan yang digunakan. Kajian ini memperkenalkan kaedah baru yang melibatkan penggunaan lapisan intumescent dengan ketebalan yang berbeza untuk menyediakan penutup penuh CSB, bertujuan untuk meningkatkan kekerasan beam apabila terdedah kepada suhu tinggi. Temuan simulasi menunjukkan bahawa penggunaan lapisan intumescent yang lebih tebal membawa kepada peningkatan marginal dalam pengurangan deformasi vertikal dan web-post buckling. Temuan ini mempunyai makna praktikal bagi profesional kejuruteraan struktural dan seni bina yang terlibat dalam reka bentuk dan penilaian struktur berasaskan keluli komposit dan bahan konkrit di kawasan-kawasan yang terdedah kepada kebakaran, menyumbang kepada kemajuan rekayasa struktural yang tahan lama.

Kata kunci: Deformasi menegak, bengkokan tiang web, suhu tinggi, dawai keluli selular (CSB), kebakaran, elemen terhingga

1.0 INTRODUCTION

Steel beams have historically played a crucial role as primary load-bearing components in the field of structural engineering, particularly in the development of flooring and roofing systems. The beams in question are essential elements that play a crucial role in composite operations, especially in the context of multi-story structures. Their interactions with concrete slabs are of utmost importance, as they contribute significantly to the overall structural integrity. Nevertheless, the ever-changing demands of building regulations and the current trends in design have given rise to novel variations of steel beams that cater to developing requirements and bring fresh opportunities.

One noteworthy advancement in recent years has been the emergence of Cellular Steel Beam (CSB), which have attracted considerable interest and implementation in the building sector as shown in Figure 1. The aforementioned beams possess a variety of noteworthy benefits, such as their visually appealing design, flexible structural components, enhanced structural integrity, and the distinctive capability to include service pipes and conduits inside the beam's web portion [13–15, 18, 19, 21, 25, 26, 35, 36]. This novel arrangement represents a notable deviation from traditional methods, since the placement of pipes and ducts is visibly situated under the flooring system, while nevertheless being integrated inside the solid steel beam [13–15, 18, 19, 21, 25, 26, 35, 36]. The accomplishment described is facilitated by an innovative engineering methodology that allows for the passage of conduits through the main web portion of these beams without affecting their structural integrity. This technology is often referred to as the Cellular Steel Beam (CSB) [13–15, 18, 19, 21, 25, 26, 35, 36].

CSB are characterized by their unique web apertures, which are typically round or rectangular in nature. These openings are carefully cut into the web sections of I or H steel beam profiles [23]. The incorporation of this novel arrangement, together with the inclusion of a concrete slab securely attached on top of the beam, has exhibited a notable enhancement in the capacity to withstand bending moments. This improvement is commonly observed to range between 50% and 100% when compared to solid steel beams [23]. In addition, CSB have a remarkable ratio of strength to weight, which enables the smooth incorporation of service utilities via the web opening [23]. The architectural uses of web opening forms are enhanced by their varied range, which includes circular, rectangular, sinusoidal, and other combinations as illustrated in Figure 2 [23]. Nevertheless, the incorporation of web openings in beams, although offering several advantages, also leads to a decrease in their load-carrying capability. This results in the emergence of multiple failure modes in the vicinity of the web opening and along the web section [13–15, 18, 19, 21, 25, 26, 35, 36].

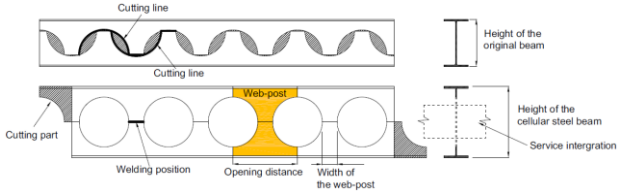

Figure 1 Cellular steel beam (CSB) with web opening [38]

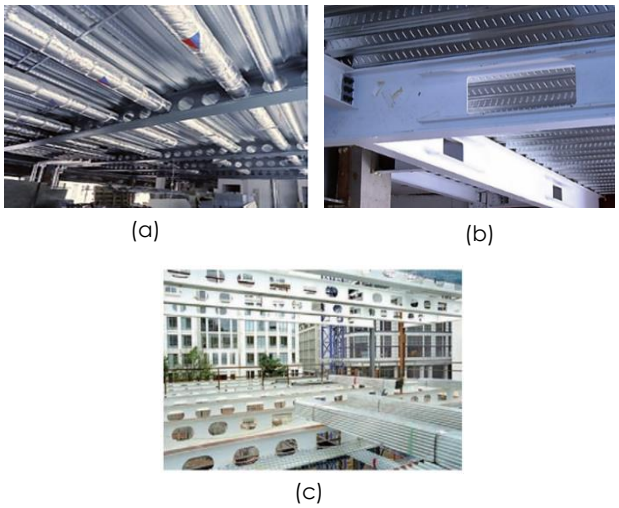

Figure 2 CSB with a common web opening shape: (a) circular, (b) rectangular, or (c) a combination of circular and rectangular [23]

The complicated nature of CSB' behavior, particularly when exposed to higher temperatures, presents sophisticated technical obstacles. Previous research has examined the effectiveness of solid steel beams and cellular steel beam (CSB) under various temperature conditions, employing both experimental and computational methods [1, 16, 27, 37, 42]. However, there are still certain areas where our knowledge is lacking. There is a significant lack of detailed design recommendations specifically addressing the structural behavior of steel beams with exposed web holes subjected to extreme temperatures [8, 9, 23]. Despite the existence of prescriptive criteria for steel beams with web apertures at ambient temperatures, the achievement of fire resistance for these beams continues to be a subject of continuous discussion among academics [2, 24]. The phenomenon of steel beams undergoing fast temperature increase during a fire incident, which frequently results in web-post buckling (Figure 3) and Vierendeel bending failure modes (Figure 4), highlights the intricate nature of this problem [17, 27, 29, 33, 34, 39].

During a fire incident, it has been observed that the Young's modulus, which represents the stiffness of a beam, experiences a quick fall in comparison to the strength of steel [9]. As a consequence, the beam's overall load-bearing capabilities are considerably compromised mostly owing to buckling rather than the steel's inherent strength. Due to these circumstances, it is possible for steel beams including web holes to encounter web-post failure prior to reaching the threshold temperature for members subjected to bending [38]. Steel beams have demonstrated a general capacity to endure significant fire exposure without failing, typically up to temperatures as high as 550°C. Limited research has been conducted on the fire resistance of shielded cellular steel beam (CSB) elements at elevated temperature conditions. Limited scholarly attention has been devoted to examining the experimental and numerical characteristics of CSB subjected to elevated temperatures in the presence of fire protection material beams [24, 30, 39]. The present study employed an intumescent coating as a fire protection material for the purpose of insulating the CSB in the event of fire exposure. The analysis of the fire resistance performance of the shielded CSB involved a thorough examination of several coating thicknesses through a parametric investigation.

Intumescent paints are extensively utilized in the United States, the United Kingdom, and several countries within Europe. The intumescent coating is comprised of two primary constituents when subjected to fire: a resin binder and a combination of chemicals that disintegrate and emit gas. Upon exposure to fire, the coating undergoes a phase transition, resulting in the liberation of a gaseous substance that induces the melting of the resin, so facilitating the formation of a safeguarding layer. The aforementioned stratum produces a substantial coating of char, serving as a protective barrier for the steel beam against the effects of fire. During the course of a routine fire test, it is common for the intumescent coating to undergo expansion ranging from 15 to 40 times its original thickness. The thickness of the intumescent coating exhibits variation based on the dimensions of the structural component, spanning a range of 0.5 mm to 5 mm.

Given the aforementioned difficulties, the present research endeavor undertakes a thorough examination of the conduct shown by CSB with web apertures, with a specific focus on the pivotal occurrence of web-post buckling failure. In addition, this study examines the effects of increased temperatures on the performance of CSB and investigates novel strategies to improve their ability to withstand fire. The investigation employs sophisticated finite element models and experimental verification to elucidate the interaction of several factors within this particular setting. The primary objective of this research is to provide significant contributions to the field of structural engineering by delivering practical guidance for the design and evaluation of structures based on cellular steel beam (CSB) materials, with a specific focus on areas susceptible to fire hazards. This undertaking signifies a notable progression in the advancement of the discipline of robust structural engineering.

Figure 3 Web-post buckling failure at elevated temperature [29]

Figure 4 Vierendeel bending failure mechanism [16, 23]

2.0 METHODOLOGY

The study involved a comprehensive analysis of Cellular Steel Beams (CSB) to assess their behavior when exposed to high temperatures, with a particular emphasis on the web-post buckling failure mode. The CSB were fabricated meticulously to accurately represent typical configurations encountered in structural applications. The constituent materials, including structural steel and concrete, were selected in accordance with established standards governing material properties [7, 9, 10]. The investigation focused specifically on CSB A2, a symmetrical unprotected composite CSB that has been extensively studied and previously subjected to experimental testing to ensure reliable validation.

The finite element model underwent thorough validation through the utilization of experimental data obtained from axially unrestrained simply supported composite CSB A2 fire tests. These tests were carried out at the University of Ulster in Northern Ireland [28]. In this study, we focused solely on the symmetrical composite CSB A2 derived from the experimental program. This decision enabled the implementation of a rigorous validation procedure [3, 29, 32].

In order to establish the dependability of our experimental endeavors, a meticulous validation procedure was undertaken, involving a comprehensive comparison of numerical analyses with the existing empirical data obtained from previous research inquiries. The essential data required for validation were acquired from fire experiments done by Nadjai et al. [29], Nadjai [32], Nadjai et al. [31], and Bake [3]. Our study specifically centered on the symmetrical unprotected composite CSB type A2, which has been extensively examined in prior scholarly investigations. The CSB were exposed to a gradual heating fire curve in line with existing norms and standards [5–7], as seen in Figure 5.

In order to obtain a thorough analysis of the structure, a wide range of instruments was carefully utilized. The instrumentation utilized in this study included of strain gauges, thermocouples, displacement transducers, and load cells. These instruments were strategically placed on and around the CSB specimens. The utilization of this methodology enabled the accurate observation of deformation, temperature progression, and load-bearing capability over the course of the trials. In order to achieve precise measurement recording, data collection systems were utilized, which were distinguished by their suitable sample rates and high-resolution capabilities.

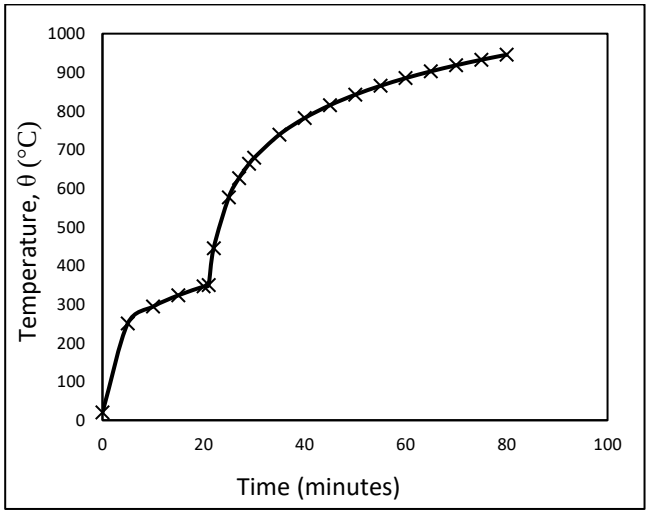

Figure 5 Slow heating fire curve BS EN 1991-1-2 and ISO 834 [7, 12, 20]

The evaluation of the non-linear characteristics of an unprotected composite CSB A2 at increased temperatures necessitated the consideration of stress-strain relationships as a fundamental factor in forecasting structural reactions. The connections presented in this study were derived using recognized standards such as BS EN 1991-1-2, BS EN 1993-1-2, and BS EN 1994-1-2 [7, 9, 10]. The steel grade utilized in the experimental trials was S355, which possesses a yield stress of 327 N/mm², as documented by Nadjai et al. [29]. The use of reduction factors was employed to consider the diminished strength and stiffness of materials when exposed to high temperatures, as mandated by the applicable standards.

The geometric properties of the composite material CSB A2 (Figure 6 (a)) were thoroughly recorded. The whole length of the beam, extending from one support to another, was measured to be 4.5 meters. The composite CSB's upper and lower Tee portions were designated as UB 406 x 140 x 39. The lower part of the tee had a final depth of 575 x 140 kg CUB, and a weight of 39 kg/m. The Composite CSB, fabricated using the S355 steel grade, was supported in a simple manner and exposed to a concentrated load. A circular aperture with a diameter of 375 mm and a center-to-center distance of 500 mm was utilized. The concrete slab possessed a thickness measuring 150 mm and a width measuring 1200 mm, exhibiting a conventional concrete grade of 35 N/mm². The concrete slab was reinforced with welded wire mesh steel with a yield strength of 460 N/mm². Shear connection studs were utilized in order to provide complete composite interaction between the lower concrete slab and the top flange of composite CSB A2. The width of the upper and lower flanges of the composite CSB A2 was measured to be 141.8 mm. The flanges had a thickness of 8.6 mm, while the web section had a thickness of 6.4 mm as illustrated in Figure (b). The spatial distribution of thermocouples along the beam section is seen in Figure 6 (c).

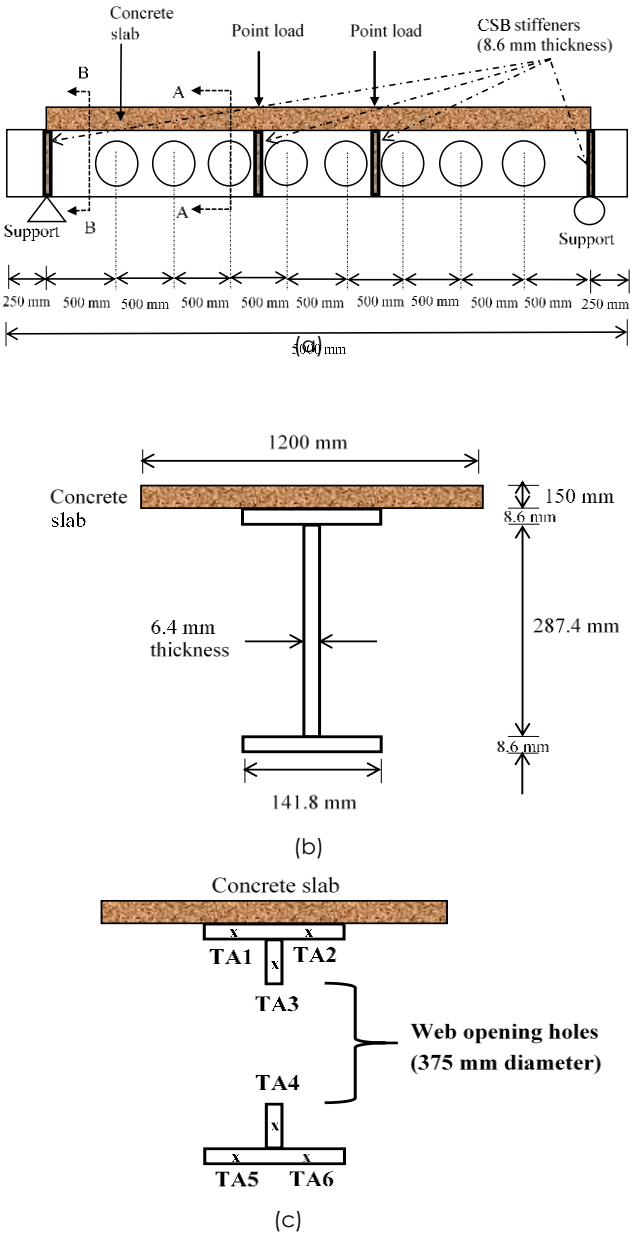

Figure 6 Detailed geometrical symmetrical composite CSB A2 shape: (a) front view, (b) cross-section viewed from B-B rectangular, and (c) thermocouple's location viewed from cross-section A-A [3, 29, 32]

In order to get a thorough analysis of the structure, a wide range of instruments was carefully utilized. The instrumentation utilized in this study included of strain gauges, thermocouples, displacement transducers, and load cells. These instruments were strategically placed on and around the CSB specimens. The utilization of this methodology enabled the accurate monitoring of deformation, temperature progression, and load-bearing capability during the conducted trials. Data collection systems were utilized, which were distinguished by their suitable sample rates and high-resolution capabilities, in order to guarantee the precise capture of measurements.

Thermocouples were strategically positioned at various locations on the composite CSB A2 in order to detect and record temperature fluctuations during the experimental procedures. Specifically, fire thermocouples TA1, TA2, TA5, and TA6 were strategically placed in the upper and lower flanges, while TA3 and TA4 were positioned in the area between the web opening and the flanges. For the purpose of verification, cross-section A-A depicted in Figure 6 was chosen. In addition, vertical deflection measurements were conducted at five discrete locations along the composite CSB A2, specifically referred to as DA1, DA2, DA3, DA4, and DA5 (as seen in Figure 7).

The experimental configuration consisted of a hydraulic testing apparatus that was carefully adjusted to impose different loading conditions on the CSB specimens. The specimens were positioned in a horizontal orientation in order to replicate their customary placement in structural settings. The experimental configuration facilitated the implementation of various loading circumstances, including both uniform and concentrated loads, so providing a full evaluation of the beams' structural response. In order to simulate heightened temperature conditions, a dedicated high-temperature furnace was utilized, which was fitted with accurate temperature control systems. These systems played a crucial role in simulating authentic fire events. The temperature profiles, which were in accordance with recognized fire curves [5–7], were carefully developed and consistently monitored throughout the experimental phase. The CSB specimens were systematically subjected to incremental temperature increments until the necessary high temperature values were achieved.

In addition to conducting experimental studies, complex finite element simulations were performed using the ABAQUS software program. The CSB specimens were subjected to a thorough modeling process, wherein painstaking attention was given to constructing detailed models that accurately represented the geometric and material aspects of the actual examples. The numerical simulations conducted in this study closely matched the experimental settings, serving two main objectives: validating the observed structural behavior and performing parametric investigations. The structural reaction of CSB was evaluated by systematically varying key parameters, including web opening diameters and intumescent coating thicknesses, in order to determine their effect.

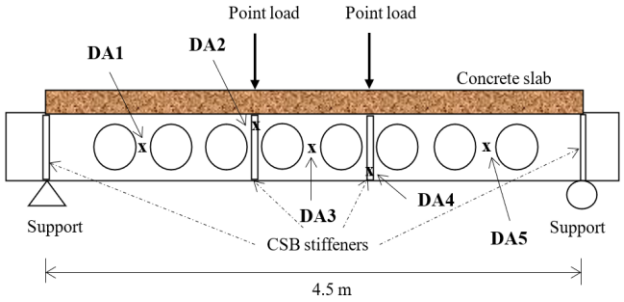

Figure 7 Measure deflection location of the composite CSB A2 [3, 29, 32]

The finite element modeling software ABAQUS was utilized to investigate the mechanical response of composite CSB A2 subjected to extreme temperatures. The heat transmission and static analyses were conducted using a finite element model that specifically included shell elements. The concrete slab was subjected to point loads at two distinct locations, mirroring the circumstances of the experimental program, as applied to the CSB. The simulations utilized transient thermal analyses to consider the temporal variation of temperature. The structural response was represented by the use of a four-node doubly curved general-purpose shell element (S4) in a simulation of finite membrane stresses. The use of the Von Mises yield criteria was employed to characterize the yield response of composite CSB A2 subjected to high temperatures.

A parametric research was done to investigate the impact of different thicknesses of intumescent coatings on the behavior of composite CSB A2 under increased temperatures after validation process were completed. The intumescent coating thicknesses used in this parametric study were 0.1, 0.3, 0.5, 1.0, 1.5, 2.0 and 5.0 mm respectively. The initial segment of the beam was coated with intumescent materials in order to evaluate their influence on the thermal behavior of the steel beam cross-section. This parametric investigation involves with the web-post buckling failure that taking into account the combined effects of heat exposure and applied vertical force. One crucial aspect of the current research work was using intumescent coatings as a means of fire protection for certain CSB specimens. The application of these coatings was carried out with great attention to detail on selected specimens, covering a range of thicknesses ranging from 0.5 mm to 5 mm. This process strictly adhered to established standards that regulate the application of coatings. The curing process of the coatings was allowed to proceed completely, hence guaranteeing consistent and even application on all surfaces of the CSB sample.

3.0 RESULTS AND DISCUSSION

3.1 Numerical Modelling of Composite CSB A2 With Abaqus Finite Element Simulation

The numerical simulation of Composite CSB A2 involves the application of finite membrane-strain analysis using fully integrated linear shell components, referred to as S4. The aforementioned methodology is utilized to forecast the structural behavior of a steel beam when exposed to the demanding conditions of fire. The rationale behind using quadrilateral shell pieces is their ability to effectively accept significant strain and deformation, which are crucial for correctly modelling the impacts of thermal and static stresses. The utilization of linear shell components is recognized, nevertheless, it is accepted that these elements require a longer processing time compared to their quadrilateral counterparts.

The inclusion of numerical integration techniques is a crucial aspect of our computational simulations. The utilization of these approaches is of utmost importance in the resolution of element stiffness matrices and subsequent derivation of displacement fields inside the finite element domain. In intricate situations, especially those that need higher-order components, the utilization of complete numerical integration methods, such as the Gaussian Quadrature technique, becomes necessary in order to accurately calculate stiffness matrices. The Gaussian Quadrature method is widely recognized for its inherent precision, flexibility to work without tightly defined intervals, and efficiency in minimizing function evaluations, making it a very successful methodology for numerical integration. In order to ensure the thorough integration of relevant functions, a careful selection and optimization process is employed to determine the position of several Gaussian points inside the analysis domain.

In the area of our numerical research pertaining to Composite CSB A2, it is essential to utilize complete integration. The decision to prioritize result accuracy is supported by the desire to get more precise outcomes, even if it may require additional processing resources. It is crucial to acknowledge that employing lower integration, despite its computing efficiency, may compromise the required degree of accuracy and may add instability to the model, as shown by the occurrence of the 'hourglass mode'.

Figures 8 display the graphical depiction of the Composite CSB A2 model. One figure illustrates the integration of a concrete slab on top of the beam, while the other figure portrays the independent configuration of the Composite CSB A2. Boundary constraints that align with the experimental program have been imposed on both ends of the unprotected Composite CSB A2. The numerical inquiry comprises two independent stages: a heat transfer analysis and a static analysis.

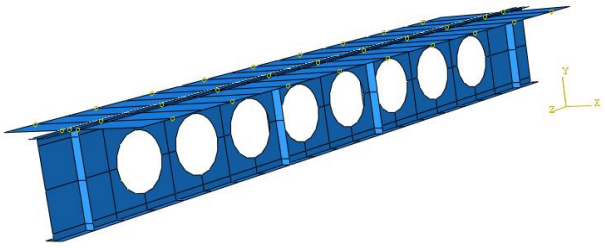

Figure 8 The composite CSB A2 model attached concrete slab on top of the beam was modelled together in ABAQUS

3.1.1 Mesh Sensitivities Analysis

Choosing the most suitable element mesh size is crucial to guarantee the precision and dependability of numerical analysis outcomes. This study conducted a thorough analysis of mesh sensitivity to identify the optimal meshing parameters for all the models examined. The model response, specifically the relationship between applied loading and vertical

deformation, was thoroughly evaluated by applying different mesh densities and corresponding global size controls. The numerical results obtained using various mesh configurations were validated by comparing them to the experimental data from previous research work [41]. The results of the mesh sensitivity analysis were used to determine the most suitable mesh for this current study. Table 1 provides a comprehensive breakdown of the number of elements and the corresponding global size control used for each model analyzed. Figure 9 illustrates the meshing results for all the models that were taken into account.

Table 1 Detailed mesh sensitivities study of SSUSB-1A model [41]

Data SSUSB-1A model							
Number of elements	1890	2538	3000	3503	4257	5076	5550
Global size control	0.05	0.048	0.045	0.04	0.035	0.032	0.03

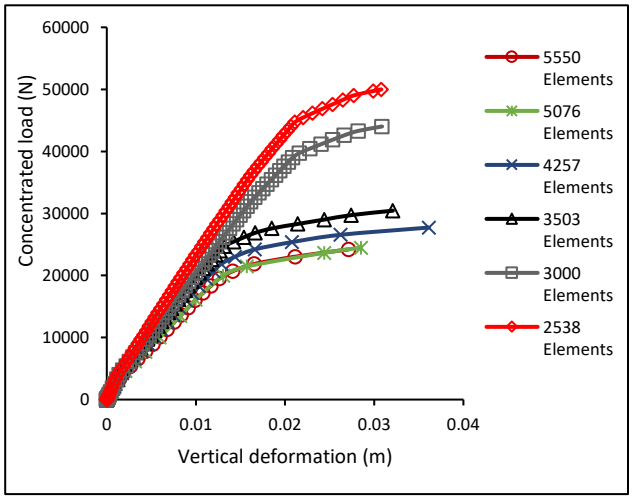

Figure 9 Mesh sensitivities analysis on SSUSB-1A model [41]

The analysis definitively determined that a mesh size of 3503 elements, which corresponds to a global size control of 0.04, is the most optimal configuration for obtaining precise and dependable numerical outcomes. Therefore, the mesh size of 3503 elements were selected and used for finite element simulation for this current reseach work.

3.1.2 Heat Transfer Analysis

The topic of fire exposure is evoked by the use of a gradual heating fire curve, as seen in Figure 5. The curve accurately replicates the fire testing circumstances seen in the experimental studies, with a fire duration of 4800 seconds. The computational framework selected for this study is transient analysis, which is well-suited for accurately capturing the time-dependent behavioral subtleties that arise in response to the applied fire exposure. The heat transfer to the steel surface is regulated by the combined mechanisms of convection and radiation. The coefficient values for convection, specifically for exposed and unexposed steel surfaces, are determined based on known design rules [7–9, 11, 23]. These codes provide quantification of heat transfer at rates of 25 W/m²K and 9 W/m²K for exposed and unexposed steel surfaces, respectively. Steel surfaces are required to have a radiation value of 0.8, as specified in design rules [7–9, 11, 23]

The thermal conductivity and specific heat values of steel and standard weight concrete are obtained from reputable design codes [7–9, 11, 23] and are smoothly incorporated into the ABAQUS simulation platform. The inclusion of a comprehensive tie constraint interaction between the unshielded Composite CSB and the concrete slab is of considerable importance. The selection of this modeling approach is motivated by the need to incorporate the behavior of post-failure concrete slabs, which is required because to the composite action shown by the unprotected Composite CSB and the concrete slab. The analysis of heat transmission is conducted using four-node linear heat transfer quadrilateral shell elements, namely the DS4 elements. This analysis is simultaneously applied to both the unprotected Composite CSB and the concrete slab.

3.1.3 Static Analysis

The following aspect of our numerical investigation involves static analysis, in which an applied load is exerted on the upper surface of the concrete slab. The Composite CSB A2 model incorporates a load magnitude of 90 kN, as referenced in relevant literature [3, 29, 32]. The nodal temperature outputs, obtained from the heat transfer analysis, are then incorporated into the static analysis framework. This integration enhances the numerical simulation's ability to examine the simultaneous behavior of the unprotected Composite CSB under both fire exposure and applied stress conditions. The temporal scope of the analysis is consistent with the heat transport analysis, including a duration of 4800 seconds.

In the context of this static analysis framework, the preferred numerical approach is general static analysis. This involves utilizing the entire Newton-Raphson method to address the non-linearities associated with the unprotected Composite CSB. The interaction mechanism remains a complete tie constraint, reflecting the conditions seen between the unshielded Composite CSB and the concrete slab. The structural behavior is simulated using S4, which refers to four-node doubly curved general-purpose shell components. The material properties of steel, including its linear elasticity and non-linear plasticity, are derived from well-established research sources [3, 22]. The modulus of elasticity values for steel and concrete are obtained from well-established design regulations [4, 9]. The stress-strain curves that illustrate non-linear behavior in steel and concrete are derived in a similar manner using design standards [4, 9]. The density of the steel beam and concrete slab are taken as 7850 and 2400 kg/m³ respectively. The concrete

damage plasticity material model is employed to mimic the non-linear plasticity behavior of the concrete slab that were extracted from standard code [4] which were based from previous reserch work [29].

3.2 Validation Results of The CSB Model

Within this particular section, we engage in the essential endeavor of model validation. Our focus is specifically on the transient heat thermal study, where the model is subjected to a 4800 second fire exposure. In order to maintain adherence to the empirical program, the strategic placement of thermocouples is employed, as seen in Figure 6. The validation process is dependent on doing a comparative evaluation of the measured and anticipated temperatures at specific locations within the Composite CSB A2 model. Significantly, the temperature measurements obtained from thermocouples positioned on the upper flange part, web section, and bottom section are compared, as seen in Figure 10. The thermocouples mentioned in this context are labeled as TA1, TA3, and TA5, indicating their placement in the top flange portion, upper and lower tee sections, and the bottom flange section of the web opening, respectively.

Figure 11 provides a graphical representation that clarifies the temperature comparisons seen at the significant monitoring sites. This figure effectively summarizes the temperature profiles obtained from the measured data and compares them with the expected values. The finite element model demonstrates a strong ability to accurately represent the temperature changes, closely matching the observed data. This provides more support for the reliability of the model.

In addition to the thermal validation, the experimental program includes the implementation of five linear variable displacement transducers (LVDTs) on the Composite CSB A2 model. These transducers are specifically used to investigate the maximum vertical deformation. The LVDTs are strategically placed along the web section and are assigned distinct identifiers, namely DA1, DA2, DA3, DA4, and DA5. The focal point of deflection analysis is located at LVDT DA3, which is strategically placed at the midpoint of the beam.

At higher temperatures, it is widely acknowledged that steel beams have a reduction in rigidity beyond a specific temperature threshold, sometimes referred to as 550°C. The critical temperature threshold in the Composite CSB A2 model is seen to occur at around 3600 seconds, which is equivalent to 60 minutes of fire exposure, as demonstrated in Figure 10. Additional examination is directed towards the LVDT DA3 (Figure 12), which displays the most notable maximum vertical deflection, measured at 0.2 meters (200 mm). Significantly, the numerical model exhibits a high degree of agreement with empirical evidence, yielding a projected maximum vertical deflection of 0.201 m (201 mm). This outcome confirms the model's coherence with experimental facts.

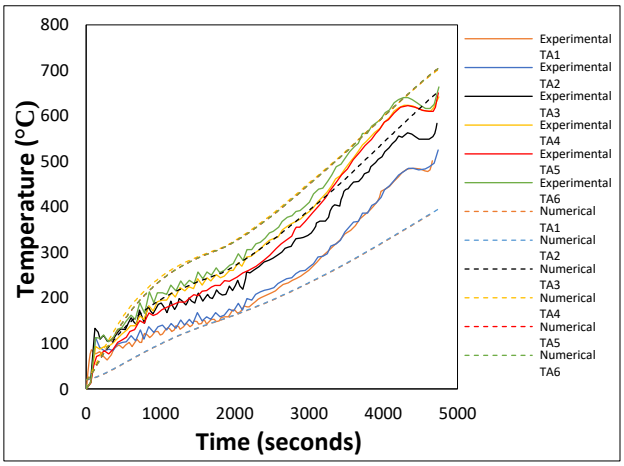

Figure 10 Measured and prediction temperature evolution of composite CSB A2 [3, 29, 30]

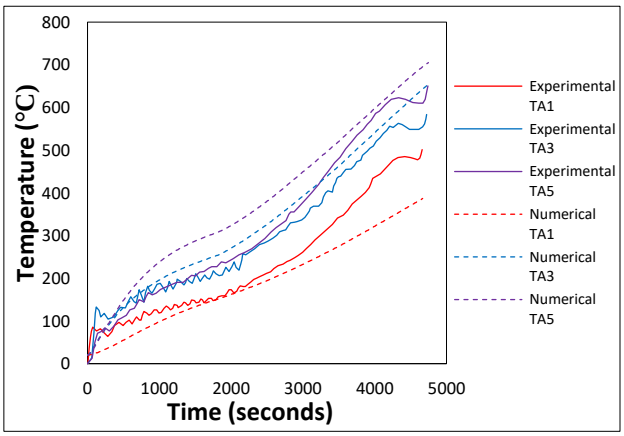

Figure 11 Comparison between the measured and predicted temperature for point TA1, TA3 and TA5 of composite CSB A2 at elevated temperature

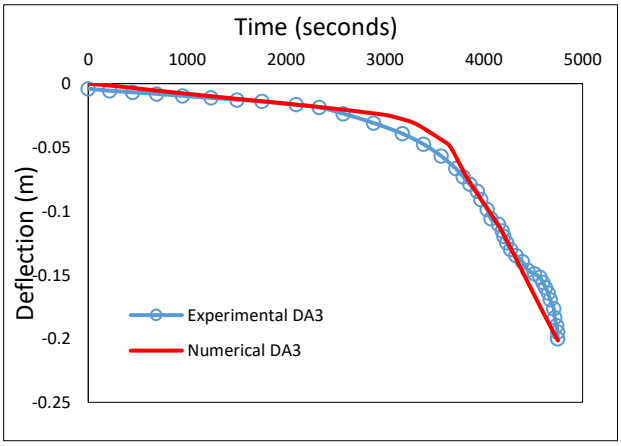

Figure 12 Comparison between the measured and predicted maximum mid-span deformation of LVDT DA3 of composite CSB A2 at elevated temperature

Figure 13 serves to emphasize the validation process, ultimately resulting in a harmonization between the empirical experiment and the numerical simulation. The provided figure presents a comparative study between the experimental test program and the numerical simulation. This comparison highlights the strong agreement between the empirical and numerical results. The harmonization also encompasses the other sites of the LVDT (DA1, DA2, DA4, and DA5), hence reinforcing the strong validity of the model.

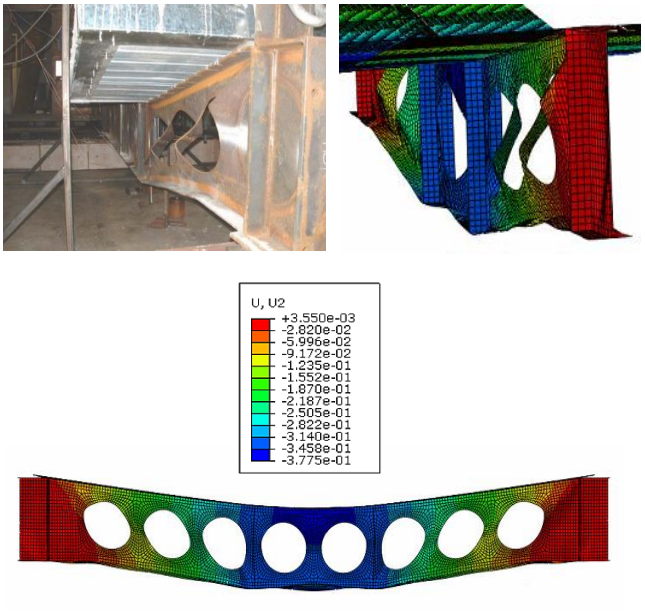

Figure 13 Comparison between ABAQUS simulation failure mode against the experimental test of composite CSB A2 [3] under fire exposure and static loading

The parametric research of the comprehensive composite CSB A2 model commenced with the overarching objective of conducting finite element simulations using ABAQUS software. The goal of these simulations was to assess the crucial failure modes associated with web post-buckling and Vierendeel bending failure mechanisms. In the present parametric research investigations, the application of a comprehensive fire protection material, namely intumescent coating, was employed on the composite CSB A2, as opposed to the validation technique used previously. The CSB A2 model was completely enveloped in an intumescent covering, as seen by the red lines in Figure 14. When varying thicknesses of intumescent coating are used, both failure types result in a decrease in lateral deformation and von Mises stress.

When subjected to elevated temperatures in the presence of a fire, intumescent coatings undergo a process of expansion, resulting in the formation of a voluminous charred residue and a reduction in density. The use of intumescent material provides additional protection to the structural steel element [22, 40]. The utilization of intumescent coatings offers several benefits, including little space occupation, expedient application, and rapid visibility of the structural steel upon application of the coating onto the steel component. Consequently, the present study will employ an intumescent coating as the fire protection layer. The aforementioned coating possesses a comparative benefit over alternative custom board solutions because to its lack of a thicker covering encompassing the CSB component. The fire exposure of composite CSB A2 with web apertures was evaluated by finite element (FE) analysis.

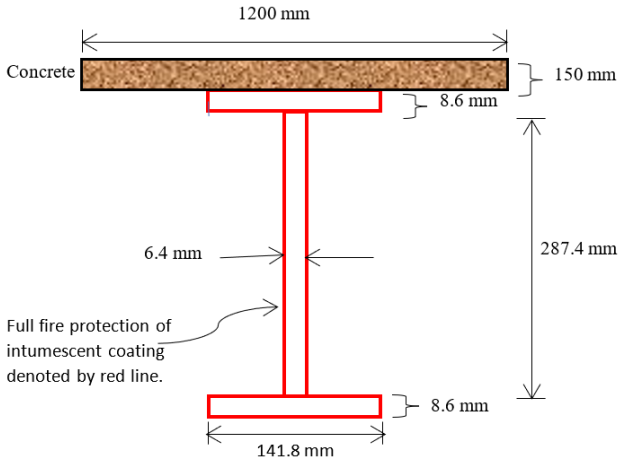

Figure 14 Cross-section view of composite CSB A2 fully wrapped with intumescent coating

3.3 Parametric Investigation of Web-Post Buckling Failure

Once the validation process has completed, parametric investigation were conducted to investigate the web-post buckling failure behaviour with various of intumescent oating thickness contraint to the surface of the steel beam. The varying intumescent coating applied were 0.1, 0.3, 0.5, 1.0, 1.5, 2.0 and 5.0 mm respectively. Figure 15 illustrates the visual representation of web-post buckling in conjunction with the composite CSB A2. The data shown in the figures illustrates that the web-post parts are denoted as WPA1, WPA2, WPA3, WPA4, and WPA5. The web-post segment of WPA4 and WPA5 exhibit similarity to that of WPA3 and WPA2 due to the symmetrical geometry of the composite beam. Figure 16 illustrates a schematic cross-section of composite steel beam CSB A2, as depicted at section A in Figure 15. This viewpoint, in accordance with the beam's length, illustrates the steel beam profile, including the web and flanges, and highlights the presence of two circular web openings. Figure 16 delineates the positions of measurement sites along the web's centerline, designated as Point 1 to Point 11. These locations are strategically located to monitor the web's dynamics, especially concerning the web openings and the vertical segments of the web

between these openings, referred to as web-posts. The numerical labels affixed to each point denote its distance, measured in millimeters, from the uppermost flange of the steel section. With a total web height of 575 mm, these precisely defined locations are crucial for establishing a direct correspondence between observed deformations, such as the web-post buckling illustrated in Figure 15, and their corresponding positions on the beam's cross-section. Figure 17 illustrates the lateral deflection behavior of the composite CSB A2 with varying intumescent coating thicknesses of 0.1 mm. Table 1 summarizes the remaining web-post deflection in conjunction with various thicknesses of intumescent coating.

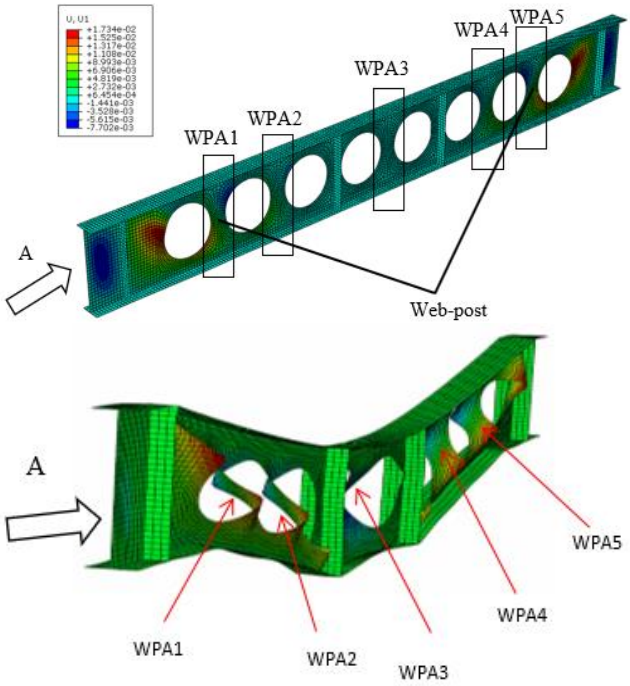

Figure 15 Web-post buckling location along with the naked composite CSB A2 at initial and 4800 seconds of fire exposure

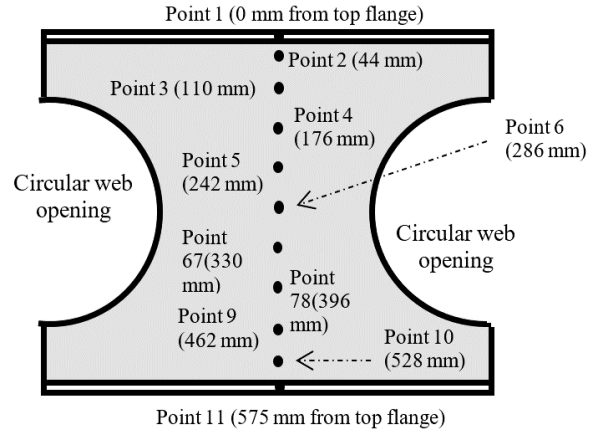

Figure 16 Measured point location for WPA1, WPA2, and WPA3 (view taken from A of Figure 17) along with the web section height of composite CSB A2

Figure 17 illustrates the greatest lateral displacement in the out-of-plane direction of a composite CSB A2 model that has been provided with an extra 0.1 mm intumescent coating, under fire exposure conditions. The web-post buckling section WPA3 exhibits the most significant lateral displacement on the left side of the protected composite CSB A2. The web-post buckling portions WPA1 and WPA2 were subsequently observed. The web-post buckling portions of WPA1 and WPA2, in contrast to WPA3, exhibit deflection in the opposite direction. The lateral displacement of the web-post buckling section WPA3 aligns with the direction of the top tee section till a vertical distance of 0.176 m downwards. The lateral deformation of the protected composite CSB A2 is influenced by the circular web opening shape present along its web section. The anticipated buckling behavior was found to be comparable when substituting a 0.1 mm thick composite CSB A2 for an uncoated composite CSB A2. At increased temperatures, the lateral deflection on the left-hand side of the web-post buckling section WPA3 reaches a maximum of 0.0762 m (76.2 mm). The web-post buckling portions of WPA1 and WPA2 exhibit deformation in a direction opposite to that of the protected composite CSB A2. At a fire exposure duration of 4800 seconds, the deflection of both sites is measured to be 0.0652 m (65.2 mm) and 0.0554 m (55.4 mm), respectively. The vertical deflection of the web-post buckling section WPA3 is limited to a maximum value of 0.33 m downwards from the top flange section of the protected composite CSB A2. When comparing the two web-post buckling sections, WPA1 and WPA2, it is seen that both sections have a maximum deflection of 0.396 m.

Table 2 presents a comprehensive overview of the maximum lateral deflection values corresponding to different coating thicknesses, namely 0.1, 0.3, 0.5, 1.0, 1.5, 2.0, and 5.0 mm. The results indicate that the lateral deformation characteristics are consistent when comparing a 0.1 mm coating thickness to thicker intumescent coatings of 0.3 mm and 0.5 mm thickness, respectively. The web-post buckling section WPA3 exhibited the highest maximum lateral distortion for both coating thicknesses of 0.3 mm and 0.5 mm. However, it should be noted that the maximum lateral deflection of both coatings exhibited an increase of 1.3 mm and 2.3 mm, respectively. Specifically, the lateral deflection values reached 0.0749 m (74.9 mm) and 0.0739 m (73.9 mm) after being subjected to a fire exposure duration of 4800 seconds. The anticipated maximum lateral distortion is 0.0903 meters (or 90.3 millimeters) and 0.089 meters (or 89 mm), in contrast to the 0.092 meters (or 92 mm) observed with a coating thickness of 0.1 mm. Moreover, the utilization of coating thicknesses of 0.3 mm and 0.5 mm leads to an enhancement in the maximum lateral displacement of the web-post buckling sections WPA1 and WPA2. When a coating thickness of 0.3 mm was applied to the web-post buckling sections WPA2 and WPA1, the maximum lateral deflection measured 0.054 m (equivalent to 54 mm) and 0.0632 m (equivalent to 63.2 mm), respectively. Both web-post buckling

sections, WPA2 and WPA1, exhibit an enhanced maximum lateral deflection of 0.0531 m (53.1 mm) and 0.0619 m (61.9 mm), respectively, after being subjected to a 4800 second fire exposure with a coating thickness of 0.5 mm.

Table 2 Summary of maximum lateral deformation of composite CSB A2 expose to 4800 seconds of fire exposure

Intumescent coating thickness (mm)	Web-post section					
	WPA1			WPA2		
	Maximum lateral deflection (mm)	Lateral deflection improves mm)	Lateral deflection improves (%)	Maximum lateral deflection (mm)	Lateral deflection improves mm)	Lateral deflection improves (%)
No coating	63.4	-	-	49.5	-	-
0.1	65.2	-1.8	-2.8	55.4	-5.9	-11.9
0.3	63.2	0.2	0.3	54	-4.5	-9.1
0.5	61.9	1.5	2.4	53.1	-3.6	-7.3
1.0	59.3	4.1	6.5	50.5	-1	-2.0
1.5	59.6	3.8	6.0	51.3	-1.8	-3.6
2.0	59	4.4	6.9	50.5	-1	-2.0
5.0	57.1	6.3	9.9	47.5	2	4.0

Intumescent coating thickness (mm)	Web-post section		
	WPA3		
	Maximum lateral deflection (mm)	Lateral deflection improves mm)	Lateral deflection improves (%)
No coating	78.2	-	-
0.1	76.2	2	2.6
0.3	74.9	3.3	4.2
0.5	73.9	4.3	5.5
1.0	72.6	5.6	7.2
1.5	71.7	6.5	8.3
2.0	71.3	6.9	8.8
5.0	71	7.2	9.2

The lateral deflection of web-post buckling section WPA1 had a marginal reduction from 0.1 mm coating thickness to 5.0 mm after being subjected to 4800 seconds of fire exposure. The maximum lateral displacement of the point web-post buckling section WPA1 is somewhat overstated when a 0.1 mm coating layer is applied, as comparison to the unprotected composite CSB A2 model. The web-post buckling section WPA1 has a maximum lateral deflection value of 65.2 mm (4800 seconds), which is 1.8 mm more than that of the unprotected composite CSB A2 model. The deflection subsequently diminishes from 0.2 mm (with a corresponding deflection of 63.2 mm), followed by 1.5 mm (with a deflection of 61.9 mm), and further lowers to 4.1 mm (with a deflection of 59.3 mm). This trend continues until it eventually rises again to around 0.3 mm, resulting in a deflection of 59.6 mm after being exposed to fire for a duration of 4800 seconds. Nonetheless, the utilization of intumescent coatings with thicknesses of 2.0 mm and 5.0 mm results in a further decrease in the anticipated maximum lateral deflection for 4.4 mm (with a deflection of 59 mm) and 6.3 mm (with a deflection of 57.1 mm) respectively.

The web-post buckling part of WPA2 has distinct performance characteristics in comparison to both WPA1 and WPA3. The overestimation of the maximum lateral deflection occurs when employing a thicker intumescent coating in comparison to an unprotected composite CSB A2 type. The protected composite CSB A2 model predicted a maximum lateral deflection of 49.5 mm. This value was compared to the following lateral deflections: 55.4 mm (with a coating thickness of 0.1 mm), 54 mm (with a coating thickness of 0.3 mm), 53.1 mm (with a coating thickness of 0.5 mm), 50.5 mm (with a coating thickness of 1.0 mm), 51.3 mm (with a coating thickness of 1.5 mm), and 50.5 mm (with a coating thickness of 2.0 mm). However, the application of a coating with a thickness of 5.0 mm results in a decrease of 47.5 mm in the lateral deflection of the web-post buckling section WPA2.

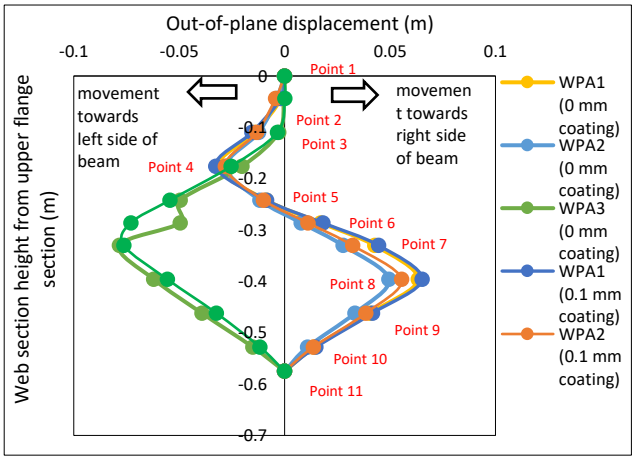

Figure 17 Lateral web-post buckling behavior of composite CSB A2 with 0.1 mm thickness of the intumescent coating at elevated temperature (viewed from A of Figure 29)

The lateral deflection characteristics of web-post buckling section WPA3 exhibit variations when compared to those of WPA1 and WPA2. In general, there is a decrease in the maximum lateral deflection seen when comparing the unprotected composite CSB A2 model to the protected composite CSB A2 model. The maximum lateral deflection exhibits a decreasing trend as the thickness of the coating increases. Specifically, the lateral deflection decreases from 78.2 mm (in the absence of any coating) to 76.2 mm (with a coating thickness of 0.1 mm), 74.9 mm (with a coating thickness of 0.3 mm), 73.9 mm (with a coating thickness of 0.5 mm), 72.6 mm (with a coating thickness of 1.0 mm), 71.7 mm (with a coating thickness of 1.5 mm), 71.3 mm (with a coating thickness of 2.0 mm), and finally stabilizes at 71.3 mm with a coating thickness of 5.0 mm. The web-post buckling section WPA3 exhibits a constant decrease

in maximum lateral deflection when compared to WPA1 and WPA2. It was hypothesized that an increase in the thickness of the intumescent coating from 0.1 mm to 5.0 mm would result in a significant enhancement in steady lateral deformation. The buckling failure of the web-post was further illustrated by the utilization of ABAQUS finite element simulation results, as seen in Figure 18.

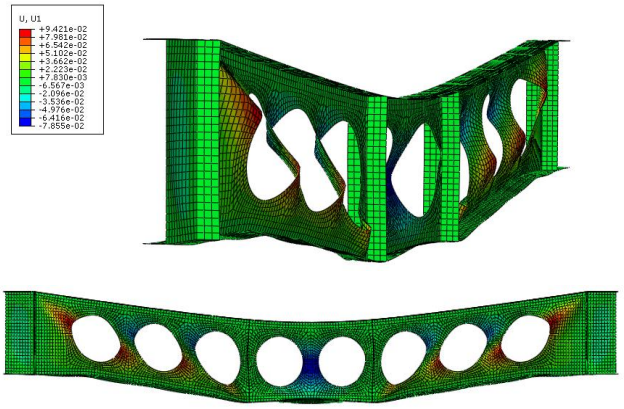

Figure 18 Web-post buckling failure through ABAQUS FE simulation output of composite CSB A2

4.0 CONCLUSION

The research used ABAQUS finite element software's many functions to accurately model the Composite CSB temperature distribution under high temperatures. This was achieved by meticulously building thermal models that included the heat conductivity values of key parts such the intumescent coating, CSB, and concrete slab. The modeling framework used shell pieces that were carefully tailored to precisely simulate protected CSB thermal behavior at high temperatures. The models were rigorously verified and validated by matching their predictions with experimental data. The analysis concepts formed the whole findings.

The symmetrical unprotected composite CSB A2 has been validated using empirical data, demonstrating its ability to precisely mimic temperature changes during fires. No intumescent coating was added to the composite beam during validation. The validation approach highlights the numerical model's accuracy in displaying fire thermal effects.

Web-post buckling in symmetrical unprotected composite CSB A2 under high temperature and applied loads has been extensively studied. The web-post segment's complex behavior was examined without considering an intumescent coating. This study's analysis helped explain structural elements' fire-induced weaknesses and deformities.

Thorough parametric analysis of symmetrical protected composite CSB A2 web-post buckling behavior is the emphasis of this work. Different intumescent coating thicknesses are tested under high temperature and vertical tension. This research is vital to our understanding of this topic. This study has clarified the composite beam's structural behavior with different thermal insulation levels. The experiment revealed complex findings on the beam's performance and deformation reduction in connection to intumescent coating thickness.

The validation of the nonlinear static model developed using the widely used ABAQUS finite element software, for the composite CSB A2 without protective measures and covered with an intumescent coating under high temperature and applied load is a significant achievement. Despite boundary restrictions and load application challenges, validation improves the model's ability to predict the largest vertical deflection. Node-based boundary conditions improve the model's predictions' fidelity.

This study explores the critical temperature threshold at which the composite CSB A2 loses stiffness without protection. Reduction happens about 550°C. This empirical validation is compatible with fire engineering knowledge, supporting the need to include fire prevention strategies in structural design to delay dangerous temperatures.

As fire protection materials, intumescent coatings minimize lateral deformations inside the web-post buckling section (WPA3), according to numerical simulations. This study shows that intumescent coatings improve composite CSB fire resistance and reduce deformation.

This study underlines the need of addressing fire consequences like lower stiffness and lateral deformations when designing and assessing composite CSB. These significant phenomena must be considered by structural engineers and designers when building structural fire safety systems. They must maintain structural integrity during fires.

To ensure finite element simulation accuracy, rigorous numerical integration technique selection, as shown by this research's preference for complete integration, is essential. Careful selection, especially for complicated structural analyses involving fire exposed composite CSB, emphasizes scientific precision.

This study provides helpful information, but more research is needed. Future study may examine other fire protection materials, structural arrangements, and beam typologies, broadening fire-resistant design paradigms. The application of this work to real-world circumstances and the assessment of practical challenges to applying these findings could make a significant contribution to structural fire engineering.

In conclusion, this research uses ABAQUS to computationally model composite CSB A2, providing insights for improved structural design and optimization in the construction sector. The study highlights the use of intumescent coatings for cost-effective fire protection, leading to enhanced building codes. Accurate long-term performance and maintenance predictions are crucial for ensuring structural integrity and durability. The research also

promotes environmental sustainability and the development of fire-resistant materials, advancing fire safety and structural durability.

Lastly, this study provides valuable insights into the behavior of composite CSB A2 under fire exposure and loading conditions. However, it also acknowledges certain limitations that present opportunities for future research. The numerical modeling may not accurately capture the intricate behaviors observed in real-world scenarios due to the assumptions and simplifications made, especially with regards to material properties and boundary conditions. Further detailed investigation is necessary to enhance the accuracy of simulations under extreme conditions, specifically regarding the temperature-dependent properties of materials like steel and concrete. Furthermore, the fire modeling methodology employed in this study, which was centered around a particular scenario, fails to encompass the ever-changing nature of fire propagation and its interaction with various structural materials. Further investigation is needed to thoroughly examine the factors that affect long-term performance, such as material degradation, fatigue, and structural integrity after a fire. Furthermore, although the study employed experimental data for initial verification, there is an acknowledged requirement for more extensive empirical examination, such as field testing on real structures, to confirm and improve the simulation outcomes. To enhance the findings and expand their relevance in the field of structural engineering and fire safety, it is imperative to address these limitations in future research.

Acknowledgement

This research was supported by School of Civil Engineering, College of Engineering, Universiti Teknologi MARA (UiTM), Shah Alam, Selangor.

Conflicts of Interest

The author(s) declare(s) that there is no conflict of interest regarding the publication of this paper.

References

[1] Altaee, M. J. *et al*. 2017. Experimental Investigation of CFRP-strengthened Steel Beams with Web Openings. *Journal of Constructional Steel Research*. 138: 750–760. Doi: https://doi.org/10.1016/j.jcsr.2017.08.023.

[2] Association for Specialist Fire Protection (ASFP) *et al*. 2004. *Fire Protection for Structural Steel in Buildings*. Third Edition (Revised June 2004). Association for Specialist Fire Protection (ASFP), Fire Test Study Group (FTSG) and The Steel Construction Institute (SCI).

[3] Bake, S. 2010. *Behaviour of Cellular Beams and Cellular Composite Floors at Ambient and Elevated Temperatures*. The University of Manchester, Manchester, UK.

[4] British Standards Institute (BSI). 2004. BS EN 1992-1-2: 2004 Design of Concrete Structures - Part 1–2: General Rules - Structural Fire Design. British Standards Institute (BSI).

[5] BSI. 1987. BS 476-20: Fire Tests on Building Materials and Structures.

[6] BSI. 2012. BS EN 1363-1:2012 Fire Resistance Tests - Part 1: General Requirements.

[7] BSI. 2002. BS EN 1991-1-2:2002 Actions on Structures — Part 1–2: General Actions — Actions on Structures Exposed to Fire.

[8] BSI. 2005. BS EN 1993-1-1:2005 Design of Steel Structures - Part 1–1: General Rules and Rules for Buildings.

[9] BSI. 2005. BS EN 1993-1-2:2005 Design of Steel Structures — Part 1–2: General Rules — Structural Fire Design.

[10] BSI. 2005. BS EN 1994-1-2:2005 Design of Composite Steel and Concrete Structures —Part 1–2: General Rules — Structural Fire Design.

[11] BSI. 2005. BS EN 1994-1-2:2005 Design of Composite Steel and Concrete Structures —Part 1–2: General Rules — Structural Fire Design.

[12] BSI. 2003. PD 7974-1: 2003. Application of Fire Safety Engineering Principles to the Design of Buildings.

[13] de Carvalho, A. S. *et al*. 2022. Assessment of Lateral–torsional Buckling in Steel I-beams with Sinusoidal Web Openings. *Thin-Walled Structures*. 175: 109242. Doi: https://doi.org/https://doi.org/10.1016/j.tws.2022.109242.

[14] Claasen, J. *et al*. 2022. Structural Behaviour of a Novel Modular Cellular Steel Beam System at Elevated Temperatures based on Large-scale Experimental Testing and Numerical Modelling. *Journal of Constructional Steel Research*. 197: 107512. Doi: https://doi.org/https://doi.org/10.1016/j.jcsr.2022.107512.

[15] Correa de Faria, C. *et al*. 2021. Lateral-torsional Buckling Resistance of Cellular Steel Beams at Room Temperature and Fire Situation. *Engineering Structures*. 237: 112046. Doi: https://doi.org/https://doi.org/10.1016/j.engstruct.2021.112046.

[16] Durif, S. *et al*. 2013. Experimental Tests and Numerical Modeling of Cellular Beams with Sinusoidal Openings. *Journal of Constructional Steel Research*. 82: 72–87. Doi: https://doi.org/10.1016/j.jcsr.2012.12.010.

[17] Ellobody, E. and Young, B. 2015. Nonlinear Analysis of Composite Castellated Beams with Profiled Steel Sheeting Exposed to Different Fire Conditions. *Journal of Constructional Steel Research*. 113: 247–260. Doi: https://doi.org/10.1016/j.jcsr.2015.02.012.

[18] Ferreira, F. P. V. *et al*. 2021. Assessment of Web Post Buckling Resistance in Steel-concrete Composite Cellular Beams. *Thin-Walled Structures*. 158: 106969. Doi: https://doi.org/https://doi.org/10.1016/j.tws.2020.106969.

[19] França, G. M. *et al*. 2022. An Appraisal of the Vierendeel Mechanism Capacity of Cellular Beams with Sinusoidal Openings. *Journal of Constructional Steel Research*. 198: 107539. Doi: https://doi.org/https://doi.org/10.1016/j.jcsr.2022.107539.

[20] ISO 1999. *ISO 834 Fire - Resistance Tests - Elements of Building Construction - Part 1*.

[21] Kang, L. *et al*. 2021. Shear behaviour and strength design of cellular beams with circular or elongated openings. *Thin-Walled Structures*. 160: 107353. Doi: https://doi.org/https://doi.org/10.1016/j.tws.2020.107353.

[22] Krishnamoorthy, R. R. 2011. *The Analysis of Partial and Damaged Fire Protection on Structural Steel at Elevated Temperature*. The University of Manchester, Manchester, UK.

[23] Lawson, R. M. and Hicks, S. J. 2011. *Design of beams with large web openings (SCI P355)*. SCI.
[24] Mesquita, L. *et al*. 2015. Intumescent Fire Protection of Cellular Beams. *X Congresso de Construção Metálica e Mista*. 1–9.
[25] Moghbeli, A. and Sharifi, Y. 2021. New Predictive Equations for Lateral-distortional Buckling Capacity Assessment of Cellular Steel Beams. *Structures*. 29: 911–923. Doi: https://doi.org/https://doi.org/10.1016/j.istruc.2020.12.004.
[26] Muhammed Jasir, T. and Raj, M. P. 2022. Numerical Investigation on Behaviour of Castellated Steel Beam in Lateral Distortional Buckling. *Materials Today: Proceedings*. 65: 3874–3880. Doi: https://doi.org/https://doi.org/10.1016/j.matpr.2022.07.172.
[27] Nadjai, A. *et al*. 2017. Fire Resistance of Axial Restraint Composite Floor Steel Cellular Beams. *Journal of Constructional Steel Research*.
[28] Nadjai, A. 2005. Performance of Cellular Composite Floor Beams at Ambient Temperature. *FireSERT Test Report*. University of Ulster.
[29] Nadjai, A. *et al*. 2007. Performance of Cellular Composite Floor Beams at Elevated Temperatures. *Fire Safety Journal*. 42(6–7): 489–497. Doi: https://doi.org/10.1016/j.firesaf.2007.05.001.
[30] Nadjai, A. *et al*. 2016. Performance of Unprotected and Protected Cellular Beams in Fire Conditions. *Construction and Building Materials*. 105: 579–588. Doi: https://doi.org/10.1016/j.conbuildmat.2015.12.150.
[31] Nadjai, A. *et al*. 2016. Performance of Unprotected and Protected Cellular Beams in Fire Conditions. *Construction and Building Materials*. 105: 579–588.
[32] Nadjai, A. 2007. Test Report for Westok Ltd-Behavior of Composite Floor Cellular Steel Beams at Elevated Temperatures. Belfast, Ulster University.
[33] Najafi, M. and Wang, Y. C. 2017. Axially Restrained Steel Beams with Web Openings at Elevated Temperatures, Part 1: Behaviour and Numerical Simulation Results. *Journal of Constructional Steel Research*. 128: 745–761. Doi: https://doi.org/10.1016/j.jcsr.2016.10.002.
[34] Najafi, M. and Wang, Y. C. 2017. Axially Restrained Steel Beams with Web Openings at Elevated Temperatures, Part 2: Development of an Analytical Method. *Journal of Constructional Steel Research*. 128: 687–705.
[35] Oliveira, V. M. de *et al*. 2022. Stability Behavior of Steel–concrete Composite Cellular Beams Subjected to Hogging Moment. *Thin-Walled Structures*. 173: 108987. Doi: https://doi.org/https://doi.org/10.1016/j.tws.2022.108987.
[36] Sayed, A. M. 2022. Numerical Study of the Effects of Web Openings on the Load Capacity of Steel Beams with Corrugated Webs. *Journal of Constructional Steel Research*. 196: 107418. Doi: https://doi.org/https://doi.org/10.1016/j.jcsr.2022.107418.
[37] Sheehan, T. *et al*. 2016. Experimental Study on Long Spanning Composite Cellular Beam under Flexure and Shear. *Journal of Constructional Steel Research*. 116: 40–54. Doi: https://doi.org/10.1016/j.jcsr.2015.08.047.
[38] Wang, P. *et al*. 2014. Practical Method for Calculating the Buckling Temperature of the Web-Post in a Cellular Steel Beam in Fire. *Thin-Walled Structures*. 85: 441–455. Doi: https://doi.org/10.1016/j.tws.2014.09.019.
[39] Wang, P. *et al*. 2015. Web-post Buckling of Fully and Partially Protected Cellular Steel Beams at Elevated Temperatures in a Fire. *Thin Walled Structures*. 1–10. Doi: https://doi.org/10.1016/j.tws.2015.02.028.
[40] Yew, M. C. *et al*. 2012. Fire-resistive Performance of Intumescent Flame-retardant Coatings for Steel. *Materials & Design*. 34: 719–724. Doi: https://doi.org/10.1016/j.matdes.2011.05.032.
[41] Zakwan, F. A. A. *et al*. 2018. A Finite Element (FE) Simulation of Naked Solid Steel Beam at Elevated Temperature. *International Journal of Integrated Engineering*. 10(9): 96–102. Doi: https://doi.org/10.30880/ijie.2018.10.09.018.
[42] Zakwan, F. A. A. *et al*. 2016. Numerical Simulation of Unprotected Solid Steel Beams at Elevated Temperatures. *Life-cycle of Engineering Systems: Emphasis on Sustainable Civil Infrastructure: Proceedings of the Fifth International Symposium on Life-Cycle Civil Engineering (IALCCE 2016), 16–19 October 2016, Delft, The Netherlands*. 210.